Journal of Drug Delivery Science and Technology 121 (2026) 108368

Contents lists available at ScienceDirect

Journal of Drug Delivery Science and Technology

journal homepage: www.elsevier.com/locate/jddst

Nanoemulsion-based strategy for azithromycin administration in pediatrics

Anna Imbriano [a], Alessandro Di Michele [b], Maria Rachele Ceccarini [a], Angela Abruzzo [c], Federica Bigucci [c], Dritan Hasa [d], Ilenia D'Abbrunzo [d], Luca Casettari [e], Costanza Fratini [e], Sara Primavilla [f], Lorenzo Tazza [a], Leonardo Tensi [a], Luana Perioli [a], Cinzia Pagano [a,*]

[a] Department of Pharmaceutical Sciences, University of Perugia, via del Giochetto 5, Perugia, 06123, Italy
[b] Department of Physics and Geology, University of Perugia, Perugia, 06123, Italy
[c] Department of Pharmacy and Biotechnology (FaBiT), Alma Mater Studiorum - University of Bologna, Via S. Donato 19/2, Bologna, 40127, Italy
[d] Department of Chemical and Pharmaceutical Sciences, University of Trieste, Piazzale Europa, 1, Trieste, 34127, Italy
[e] Department of Biomolecular Sciences, School of Pharmacy, University of Urbino Carlo Bo, Via Ca le Suore 2, Urbino, PU, 61029, Italy
[f] Istituto Zooprofilattico Sperimentale dell'Umbria e delle Marche "Togo Rosati", Via Salvemini 1, Perugia, 06126, Italy

ARTICLE INFO

Keywords:
Azithromycin
Nanoemulsion
Oral delivery
Experimental design
Stability
Antimicrobial activity

ABSTRACT

Azithromycin (AZM) is a macrolide widely prescribed in pediatrics and is characterized by low solubility and bitterness. In this study, a dual-surfactant oil-in-water (O/W) nanoemulsion was optimized to overcome these limitations. High-Power Ultrasonic technique was used for emulsion production, using pumpkin seed oil as the internal O phase. At the same time, soy lecithin, a biodegradable and biocompatible phospholipid, was combined with Soluplus®, a high-molecular-weight amphiphilic polymer, to form a synergistic surfactant system. The O/W composition was optimized by a D-optimal experimental design to assess the influence of oil, surfactant and water percentages on droplet size, polydispersity index (PDI) and ζ-potential. The optimized formulation exhibited submicron droplet size (≈800 nm), low PDI (<0.08) and ζ-potential around −20 mV. Hydrophilic bentonite nanoclay was added to the final nanoemulsion, obtaining a product that remained physically stable for at least three months at 25 °C. The antimicrobial activity of the prepared nanoemulsion was confirmed by the agar diffusion method on four Gram-positive bacteria. Moreover, the time-kill test carried out on *S. aureus* showed that the nanoemulsion is active at a concentration of 23 μg/mL *vs* 400 μg/mL of the commercial suspension. A preliminary experiment, aiming to evaluate AZM interaction with the specific receptor (TAS2R4) for bitter taste perception, showed the nanoemulsion's ability to reduce AZM binding to the receptor, probably due to the combination of AZM confinement in the droplet and bentonite presence in the formulation, suggesting its potential as a valuable alternative for AZM oral administration.

1. Introduction

Azithromycin (AZM) is a broad-spectrum macrolide antibiotic widely prescribed for respiratory, skin, and soft tissue infections, particularly in pediatrics [1]. Reports from the Italian Medicines Agency (AIFA) indicate a steady increase in the prescription of AZM, one of the 10 most used antibiotics. This trend is particularly evident in the pediatric population, where macrolides, and in particular AZM, are among the most frequently prescribed antibiotic classes [2,3] due to its efficacy against many infections and tolerability. The most common side effects are gastrointestinal; however, among AZM macrolides, it is generally well tolerated [4]. Clinical studies have shown a lower incidence of side effects than other antibiotics, such as erythromycin [5]. Due to its high lipophilicity and poor aqueous solubility, responsible for a limited oral bioavailability (~37%), AZM is classified as a class II drug in the Biopharmaceutics Classification System (BCS) [6,7] (see Scheme 1).

Tablets and suspensions (200 mg/5 mL) are the only AZM-based oral formulations available on the market. Suspension is generally preferred for children 6<years old due to the versatility of both dosing and administration [8]; however, this formulation presents some critical issues. The low solubility/permeability of AZM represents a problem, especially when the drug is administered as a solid dosage form. The drug's solid particles dissolve slowly and incompletely after contact with the biological fluids. This means that the administered dose is partially absorbed, as demonstrated by the well-documented low bioavailability (~37%) [6,7]. The undissolved drug remains in the GI tract and could be

* Corresponding author. Department of Pharmaceutical Sciences, University of Perugia, Italy.
E-mail address: cinzia.pagano@unipg.it (C. Pagano).

https://doi.org/10.1016/j.jddst.2026.108368
Received 29 December 2025; Received in revised form 15 April 2026; Accepted 23 April 2026
Available online 24 April 2026

responsible for serious modifications/interactions with the gut microbiome, leading to an increase in macrolide-resistant bacteria [9].

Together to this, the use of suspensions makes difficult the correct dosing as: i) the caregiver must re-constitute the suspension before using it, as there may be mistakes in the amount of water added for the powder suspension (risks of overdosing or under-dosing); ii) the suspension must be shake before use (incorrect shaking exposes to incorrect dosing); iii) necessity of refrigeration after reconstitution, these formulations are stable only for 7-10 days, the remaining formulation must be disposed; iv) bitter taste. Literature data documents that the bitter taste of medicines (mainly antibiotics, such as azithromycin [10]) is responsible for reduced compliance, especially in pediatrics, contributing to reduced adherence to the therapy. Recent studies demonstrate that the bitter taste is one of the main reasons for medication refusal in pediatrics [11, 12]. It is well known that AZM's bitter taste perception is due to the activation of the bitter taste receptors (T2Rs), TAS2R4 subtype, resulting in pronounced bitterness that is perceived as disgusting and therefore not always well accepted, especially by children [13]. The most common taste-masking strategies used for liquid formulations (suspensions) are sweeteners and/or flavouring agents, sometimes unsuccessful. Strategies purposed to improve AZM acceptability are for example: i) nanocapsulation using coating agents (such as titanium dioxide) [14], ii) microencapsulation using polymers (e.g. Eudragit EPO and S-100) insoluble in the mouth [15], iii) complexation for example with cyclodextrins [16], iv) encapsulation into micelles or self-emulsifying drug delivery systems [17,18], v) solid dispersions [19].

Another interesting strategy, not yet investigated for pediatric dosage forms, is represented by oil-in-water (O/W) nanoemulsions. These systems are characterized by small droplet size and kinetic stability, which offer several advantages from a biopharmaceutical perspective, such as improved dissolution rate/absorption, and enhanced oral bioavailability by providing a large interfacial surface between the oil and the aqueous phase [20]. Moreover, the drug's confinement in the oil droplets could limit the contact with the papillae, resulting in a better taste perception.

The use of biocompatible and biodegradable excipients, such as natural oils and phospholipid-based surfactants, can enhance the nanoemulsions' safety profile, improving their suitability for pediatric administration. Nanoemulsions can be prepared by high-energy methods, allowing efficient emulsification and droplet size reduction. Among the high-energy methods available, the High-Power Ultrasonic technique (HPU) is a simple, efficient, and time-saving technique that can obtain a stable nanoemulsion in a very short time. HPU is an efficient method for this purpose as it exploits the principle of cavitation, consisting of the formation of microbubbles and their collapse, with subsequent breakage of the original droplets under micron size [21]. It was observed that the HPU method allows the use of a low surfactant amount compared to the other methods, which results in the formation of stable and homogenous nanoemulsions obtained in short preparation times [22].

Taking into consideration all these assumptions, this work aimed to develop and optimize a dual-surfactant oil-in-water (O/W) nanoemulsion for AZM oral administration by exploiting HPU. For this purpose, the combination of soy lecithin and Soluplus®, as a synergistic surfactant system, was explored for the first time. Soy lecithin represents an attractive surfactant due to its natural origin, biodegradability and biocompatibility. Its amphiphilic structure enables the formation of stable nano-sized droplets, maintaining safety and tolerability suitable

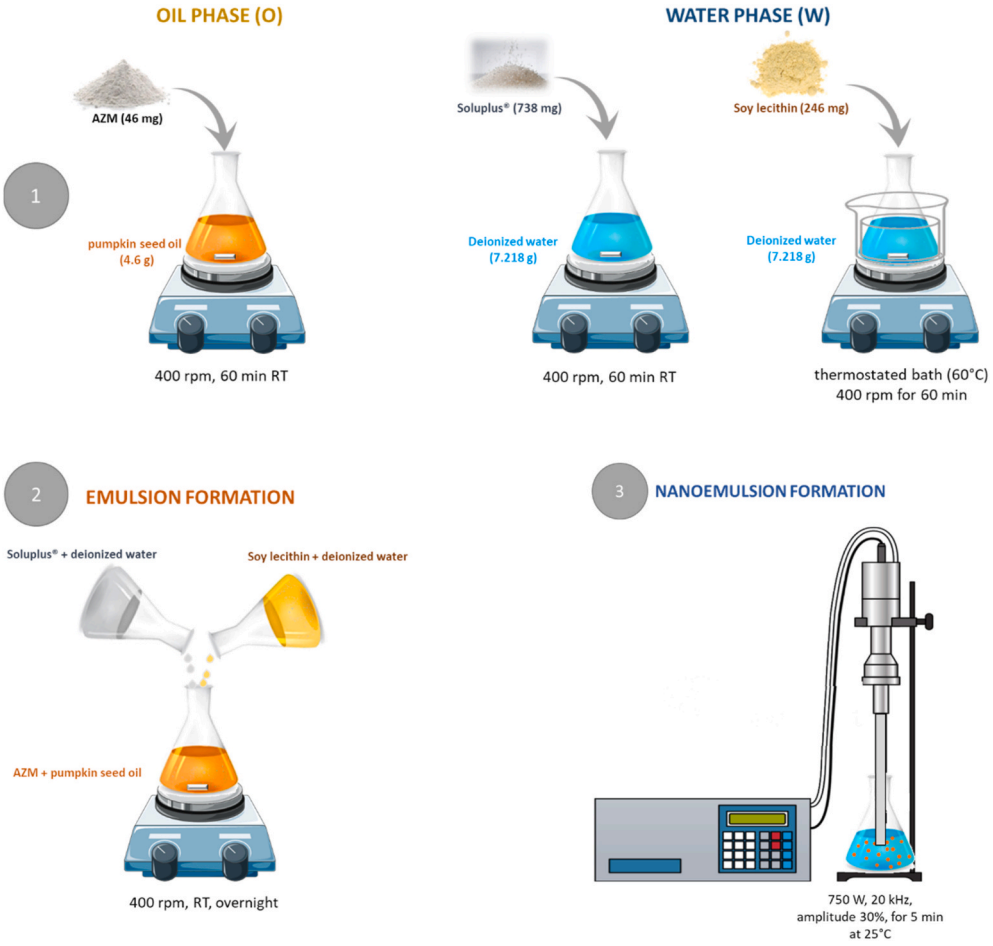

Scheme I.

for pediatric use [23,24]. As lecithin alone may not provide sufficient stabilization under dynamic stress, its combination with the amphiphilic polymeric surfactant Soluplus®, a polyvinyl caprolactam–polyvinyl acetate–polyethylene glycol graft copolymer, was considered useful. Soy lecithin and Soluplus® can create a synergistic effect, allowing the use of reduced surfactant concentrations compared to conventional low-molecular-weight surfactants [25–27].

The combination of soy lecithin and Soluplus® offers a promising "dual-surfactant" system capable of producing a stable nanoemulsion. A D-optimal experimental design approach was used to optimize the formulation properties in terms of droplet size, distribution and drug content. The introduction of the hydrophilic bentonite nanoclay in the formulation was considered useful as an agent that can physically prevent AZM interaction with the taste receptors, making the formulation more acceptable. Stability studies were performed under accelerated and long-term conditions at 4 °C, 25 °C and 40 °C for 90 days; the antimicrobial activity was studied as well. Considering that AZM bitter taste perception is due to its interaction with TAS2R4 receptors on the tongue, an *in vitro* experiment was planned. The aim was to perform a preliminary evaluation of the formulation's ability to decrease the AZM-TAS2R4 receptor interaction.

2. Materials and methods

2.1. Materials

Azithromycin dihydrate (AZM), ethanol (EtOH, 96% v/v), and hydrophilic bentonite nanoclay were obtained from Merck S.p.A. (Milano, Italy). Soluplus® was kindly provided by BASF SE (Ludwigshafen, Germany). Soy lecithin powder was purchased from A.C.E.F. S.p.A. (Fiorenzuola d'Arda, Italy). Pumpkin seed oil, wheat germ oil, and flaxseed oil were obtained from AAkon (Milano, Italy). Hydrochloric acid 37% v/v (HCl) was purchased from Carlo Erba Reagents Srl (Cornaredo, Italy). Ultrapure water was produced by reverse osmosis using a Milli-Q system (Millipore, Roma, Italy). The commercial suspension of AZM (200 mg/5 mL) was purchased in a pharmacy.

All other chemicals and solvents were of analytical grade and used without further purification. Simulated gastric fluid (SGF, pH 1.2) was prepared according to European Pharmacopoeia 11th Ed. (Ph. Eur. 11th Ed.), containing 2 g NaCl and 80 mL of 1 M HCl diluted to 1000 mL with ultrapure water; Simulated Intestinal Fluid (SIF, pH 6.8) was prepared using KH_2PO_4 0.2 M, adjusting the pH using NaOH 5 M.

Reference bacterial strains were purchased from Microbiologics (St. Cloud, MN, USA). Mueller-Hinton agar (MHA) and Mueller-Hinton agar with 5% defibrinated sheep blood (MHAB) were obtained from Oxoid Limited (Basingstoke, UK). Mueller-Hinton broth (MHB) was purchased from Biolife Italiana S.r.l. (Milano, Italy), and blood agar (BA) plates from VWR International S.r.l. (Milano, Italy).

2.2. Quantitative analysis of AZM

AZM quantification was carried out by UV–Vis spectrophotometry according to the method described by Sultana et al. [28]. Briefly, AZM dihydrate (11 mg) was dissolved in 10 mL EtOH and diluted with 10 mL ultrapure water or SGF, obtaining a final concentration of 0.55 mg/mL 8 mL of this solution was mixed with 42 mL of HCl to obtain the stock acid solution, kept at room temperature (RT) for 90 min. Absorbance was measured at 486 nm using an Agilent 8453 UV–Vis spectrophotometer (Agilent Technologies, Germany). Two calibration curves were made: i) in EtOH/water (50:50 % v/v), $R^2 = 0.99$; ii) in SGF, $R^2 = 0.99$.

2.3. Solubility studies

AZM dihydrate (250 mg) was dispersed in 5 mL of pumpkin seed oil, wheatgerm oil, or flaxseed oil and stirred at 400 rpm for 24 h at RT. Samples were centrifuged at 4000 rpm for 10 min. The supernatant (3 mL) was transferred into a dialysis bag (MWCO 12 – 14 kDa, Slide-A-Lyzer, Thermo Scientific, Mexico) and immersed in 200 mL EtOH/water (50:50 % v/v) solution. At 24, 48, and 72 h, 1.6 mL of dialysate was withdrawn and replaced with fresh EtOH/water (50:50 % v/v) solution. AZM content was determined as described in Section 2.2.

2.4. Experimental design

Nanoemulsion compositions were optimized using MODDE 13 software (Sartorius Data Analytics) with a D-optimal design comprising 11 experiments, including three centre points. Soy lecithin (SL) and Soluplus® (Sol) were employed as surfactants in the fixed ratio 1:3 (w/w) SL:Sol. The independent variables (factors) were the % of surfactant, oil, and water, whereas the mean droplet diameter and polydispersity index (PDI) were selected as responses.

Two design ranges were done: Design 1 i) surfactant (4–23% w/w), oil (4–23% w/w), water (54–92% w/w) (Table 1), ii) design 2: surfactant (4–5% w/w), oil (23–41% w/w), water (54–73% w/w) (Table 2). Experimental data were elaborated using multiple linear regression (MLR) and response surface methodology (RSM) to evaluate the effect of individual factors and their interactions on droplet characteristics. Model significance was assessed by analysis of variance (ANOVA), and the model's predictive power was estimated through R^2, Q^2, and reproducibility values provided by the software. The optimized formulation was selected based on the lowest predicted PDI and the smallest droplet size within the experimental design space.

2.5. Nanoemulsions preparation

The nanoemulsion was prepared as follows: oil phase (O): AZM dihydrate (amount corresponding to 46 mg of anhydrous form) was solubilized in pumpkin seed oil (4.6 g) and stirred at 400 rpm for 60 min at RT; water phase (W): Sol (738 mg) was solubilized in water (7.218 g) under magnetic stirring 400 rpm for 60 min at RT, SL (246 mg) was solubilized in another flask in water (7.218 g) in a thermostated bath (60 °C) under magnetic stirring 400 rpm for 60 min. Afterwards, the two aqueous phases, namely cooled SL and Sol solutions respectively, were added to the oily phase under magnetic stirring and maintained overnight at 400 rpm at RT. The obtained pre-emulsion was sonicated using a high-power ultrasonic processor by a Horn Type ultrasonic probe VCX750 (SONICS, Newtown, Connecticut, USA) operating at 750 W, 20 kHz, amplitude 30%, for 5 min at 25 °C. Hydrophilic bentonite nanoclay (NHB) was added to the prepared nanoemulsion under magnetic stirring (400 rpm). The preparation procedure is summarized in Scheme I.

2.6. Particle size and ζ-potential analysis

Particle size distribution and ζ-potential were measured by a Nicomp 380 ZLS analyzer (Santa Barbara, CA, USA). Samples were diluted with

Table 1
Nanoemulsion compositions generated from the first Experimental design (Design 1).

Sample	Surfactant (w/w %)	Water (w/w %)	Oil (w/w %)
N1	23.0	54.0	23.0
N2	4.0	92.0	4.0
N3	23.0	73.0	4.0
N4	4.0	73.0	23.0
N5	4.0	82.5	13.5
N6	23.0	63.5	13.5
N7	13.5	82.5	4.0
N8	13.5	63.5	23.0
N9	13.5	73.0	13.5
N10	13.5	73.0	13.5
N11	13.5	73.0	13.5

Table 2
Emulsions generated from the second Experimental design (Design 2).

Sample	Surfactant (w/w %)	Water (w/w %)	Oil (w/w %)
N1	5.0	54.0	41.0
N2	4.0	73.0	23.0
N3	5.0	72.0	23.0
N4	4.0	55.0	41.0
N5	4.0	64.0	32.0
N6	5.0	63.0	32.0
N7	4.5	72.5	23.0
N8	4.5	54.5	41.0
N9	4.5	63.5	32.0
N10	4.5	63.5	32.0
N11	4.5	63.5	32.0

ultrapure water until the count rate was within the instrument's optimal range. Results were expressed as mean ± SD (n = 5).

2.7. UHPLC-MS analysis

AZM integrity in the prepared nanoemulsion was evaluated using an Agilent 1290 Infinity II UHPLC coupled to an Agilent 6560 QTOF mass spectrometer (Agilent Technologies, Santa Clara, CA, USA). Chromatographic separation was achieved on a ZORBAX RRHD Eclipse Plus C18 column (50 mm × 2.1 mm, 1.8 μm). UHPLC eluent A was water (LC-MS grade, LiChrosolv, Supelco) with 0.01% (v/v) formic acid (LC-MS grade, LiChropur, Supelco) and 0.1 mM ammonium formate (LC-MS grade, LiChropur, Supelco), eluent B was acetonitrile (LC-MS grade, LiChrosolv, Supelco). The optimized gradient program was the following: 0-1 min, 5% (v/v) B; 1-4 min, 5-15% (v/v) B; 4-7 min, 15-97% (v/v) B; 7-8.5 min, 97% (v/v) B; 8.5-10 min, 97-5% (v/v) B; 10-13 min, 5% (v/v) B (column equilibration/conditioning). The column temperature was set at 25 °C using a flow rate of 0.3 mL min^{-1} and an injection volume of 5 μL. For MS detection, the Dual AJS ESI source operated in positive ion mode. The Gas temperature was set at 300 °C with a flow of 5 L min^{-1}, while the Sheath Gas Temperature was 350 °C with a flow of 11 L min^{-1}. The nebulizer pressure was set at 35 psi, and the Capillary and Fragmentor voltages were 3500 V and 400 V, respectively. The Masshunter Workstation Data Acquisition 10.0 (Agilent Technologies Inc., Santa Clara, California, United States) program was used for data acquisition, while the Masshunter Qualitative Analysis 10.0 (Agilent Technologies Inc., Santa Clara, California, United States) software was used for data processing. For the analysis, the sample was prepared as follows: 3 mL of the nanoemulsion was placed in a dialysis bag (MWCO 12 – 14 kDa, Slide-A-Lyzer, Thermo Scientific, Mexico) and put in contact with 200 mL of a water/MeOH (50:50 v/v) mixture. After 1, 2, 5, 7 and 9 days, aliquots were withdrawn and analyzed. Calibration curves (1.0 μg/mL–0.2 μg/L) were prepared daily in MeOH with triplicate measurements showing high linearity and reproducibility. Samples were diluted 35-fold with MeOH before analysis.

2.8. Optical microscope analysis

Nanoemulsion droplets were observed by a Nikon Eclipse 80i optical microscope (Melville, LA, USA).

2.9. Transmission Electron Microscopy (TEM)

The morphology of the droplets was observed by Transmission Electron Microscopy (TEM, Philips CM10, Philips Electron Optics, Eindhoven, The Netherlands). The nanoemulsion was diluted 1:50 (v/v) with bidistilled water before the analysis. The sample was positioned on carbon film nickel grids (EM-Tec Formvar 400 square mesh). Phosphotungstic acid (1% v/v) was used for negative stain, then washed with water, followed by drying for 24h. Samples were scanned at different magnification ranges with an accelerating voltage of 100 kV.

2.10. Stability studies

The physical stability of the optimized nanoemulsion was assessed through both accelerated stress tests and long-term storage stability studies. For accelerated stress tests, samples were subjected to the following conditions to evaluate their mechanical and thermal robustness: i) centrifugation: 5 mL of the formulation were centrifuged at 4000 rpm for 30 min at RT to detect potential phase separation/creaming phenomena, ii) heating–cooling cycles: samples were alternatively stored at 4 °C and 40 °C for 48 h at each temperature; this cycle was repeated three times to simulate temperature stress, iii) freeze–thaw cycles: samples were stored at −20 °C for 48 h and subsequently at RT for 48 h. This cycle was also repeated three times to assess stability under freezing conditions. After each cycle, the nanoemulsions were visually inspected for phase separation, creaming, cracking, colour changes, or gas formation, which are typical indicators of emulsion destabilization [20].

For long-term stability evaluation, nanoemulsion samples were stored in tightly sealed vials under three temperature conditions (4 °C, 25 °C and 40 °C) for 90 days. At predetermined time points (30, 60, and 90 days), samples were analyzed for hydrodynamic diameter (HD), polydispersity index (PDI), and ζ-potential using dynamic light scattering (DLS) to monitor potential changes in droplet size distribution and surface charge over time.

2.11. Stability in SGF

The stability of AZM in the developed nanoemulsion AZM_N*_NHB was evaluated in SGF, pH 1.2. Briefly, 1.5 mL of nanoemulsion was mixed with SGF (ratio 1:1 v/v) and magnetically stirred (350 rpm) at 37 °C for 30 min to simulate the gastric transit time [29]. After incubation, the system was neutralized to pH 7.0 using 5 M NaOH to mimic transit to intestinal conditions [30]. Subsequently, 3 mL of the neutralized dispersion was transferred into a dialysis membrane (Slide-A-Lyzer®, MWCO 12–14 kDa, Thermo Scientific, Mexico) and immersed in 150 mL of a water/EtOH mixture (50:50 v/v) under sink conditions. At predetermined time points (1, 2, 5, 7, and 9 days), aliquots were withdrawn and analyzed according to the procedure described in Section 2.2.

2.12. In vitro release studies

In vitro release studies were performed using the dialysis bag method. Briefly, 3 mL of nanoemulsion were placed into a dialysis membrane (Slide-A-Lyzer®, MWCO 12–14 kDa, Thermo Scientific, Mexico) and immersed in 150 mL of a mixture of SIF/EtOH (80:20 v/v). The system was maintained under constant stirring (350 rpm) at 37 °C. At predetermined time intervals, aliquots were withdrawn and immediately replaced with an equal volume of fresh release medium to maintain sink conditions. AZM concentration was determined by UV spectrophotometry (n = 3, mean ± SD) as described in section 2.2. For comparison purposes, an AZM water suspension at the same concentration as the nanoemulsion (2.3 mg/mL) was prepared and submitted to the release studies following the procedure described above.

2.13. Antimicrobial activity

The antimicrobial activity was first evaluated by agar well diffusion assay [31]. Four Gram-positive strains were tested and incubated according to the growth conditions reported in Table 3. An initial suspension of 0.5 McFarland in 0.9% sterile saline solution was prepared for each strain, and 100 μL was spread on MHA plates by a swab, except for *S. pyogenes* and *C. perfringens,* where MHAB plates were used. Fifty μL of the test samples were put into 7 mm wells. Plates were incubated under appropriate conditions (Table 3), and the inhibition zones were measured after incubation. Sterile demineralized water was used as a

Table 3
Strains used for the assay and growth conditions. Diameter of growth inhibition (in mm).

Strain	Growth conditions	Negative control - (H_2O)	Positive control – commercial suspension	AZM_N*_NHB	N* (unloaded nanoemulsion)
Staphylococcus aureus WDCM 00034	37 °C for 24 h on MHA	-	37.3 ± 0.2	21.5 ± 0.2	-
Staphylococcus epidermidis WDCM 00036	37 °C for 24 h on MHA	-	47.2 ± 0.1	28.7 ± 0.1	-
Streptococcus pyogenes ATCC 19615	37 °C for 24 h on MHAB	-	40.3 ± 0.3	30.2 ± 0.1	-
Clostridium perfrigens WDCM 00007	37 °C for 24 h under anaerobic conditions on MHAB	-	26.5 ± 0.1	15.9 ± 0.2	-

negative control.

The time-kill assay was performed against *S. aureus* WDCM 00034 following the procedure reported in a previous work [32]. AZM_N* and the commercial suspension (dilution 1:100 v/v) were incubated in broth culture (1×10^5 CFU/mL), untreated strain was used as a control. Bacterial counts (CFU/mL) were determined after 4, 8, 24 and 48 h by serial dilution and plating on BA plates and the number of CFU/mL was calculated using equation (1), as described in ISO 7218:2007 (Eq. (1)):

$$N = \frac{\sum C}{V*1.1*d}$$

$\sum C$ = is the sum of the colonies counted on the two dishes from two successive dilutions; V = is the volume (mL) of inoculum placed in each dish; d = is the dilution corresponding to the first dilution retained.

2.14. In vitro evaluation of AZM binding to TAS2R4 protein

The Human Taste Receptor Type 2 Member 4 (TAS2R4) ELISA Kit (96 Tests), purchased from MyBioSource Inc (San Diego, USA), was properly modified and used following the manufacturer's protocol. A calibration curve was obtained using the standard protein TAS2R4 provided in the kit (concentration range 112.5 – 1800 ng/L, $R^2 = 0.92$). Then, solutions of different samples in the presence of TAS2R4 protein (provided in the kit) were prepared. The tested samples were: i) sucrose as a negative control, ii) AZM as a positive control, iii) AZM_N*_NHB. Three concentrations (225, 450 and 900 ng/mL) of each sample were incubated with three TAS2R4 concentrations (225, 450 and 900 ng/mL) and kept in contact for 45 min at 37 °C, then incubated with the antibody for 30 min at 37 °C. After that, the chromogen solution necessary to detect the optical density (OD) at $\lambda_{max} = 450$ nm was added. The results are expressed by OD measured by a multimode plate reader (Microplate Reader Infinite M Plex 200 Pro TECAN).

2.15. Statistical analysis

Experimental design data were analyzed using MODDE® Pro software. A D-optimal design and Partial Least Squares (PLS) regression were applied. Model adequacy was assessed by ANOVA using p-values ($p < 0.05$). Goodness-of-fit and predictive performance were determined using R^2 and Q^2 parameters. Model validity, reproducibility, and lack-of-fit tests were also considered. Results are reported as mean ± SD.

3. Results and discussion

3.1. O/W emulsion composition optimization

The first stage of O/W nanoemulsion development consisted of the identification of the most suitable oil phase capable of dissolving the largest possible amount of AZM. In fact, the maximization of drug amount solubilized in the internal phase is essential to achieve high drug loadings, reduce precipitation risks and ensure uniform drug distribution within the final nanoemulsion droplets [33]. Considering these aspects, three vegetable oils, namely pumpkin seed oil, wheat germ oil, and flaxseed oil, were considered. Each oil was selected for its recognized biocompatibility and potential antioxidant contribution, which may further enhance formulation performances. The measured AZM solubility in the selected oils was: 11.85 ± 0.07 mg/mL in pumpkin seed oil, 11.37 ± 0.08 mg/mL in wheat germ oil and 9.86 ± 0.07 mg/mL in flaxseed oil. AZM content was determined by the method reported in Section 2.2. The best solubilizing ability was achieved with pumpkin seed oil, possibly because of its balanced composition of triglycerides and unsaturated fatty acids. This could be responsible for a favourable lipophilic environment useful for AZM dissolution [34]. Based on these findings, pumpkin seed oil was selected as the internal oil phase for subsequent formulation steps.

A D-optimal experimental design was performed using MODDE® 13 software to develop a stable nanoemulsion with optimal drug loading and droplet size. Pumpkin seed oil represented the oil phase, while Soluplus® (Sol) and soy lecithin (SL) were used as surfactants in a ratio of 1:3 w/w (SL:Sol).

Sol, a polyvinyl caprolactam–polyvinyl acetate–polyethylene glycol graft copolymer (MW ≈ 118,000 g/mol; HLB 14), was chosen for its dual role as a polymeric surfactant and solubilizing agent for poorly soluble drugs, well documented in literature [27]. The admitted safe amounts are up to 8000 mg/day for adults and 30 mg/kg for pediatric patients [35]. SL, mainly consisting of phosphatidylcholine and other phospholipids, is a natural, biodegradable emulsifier widely used in both food and pharmaceutical industries owing to its safety and bioavailability-enhancing properties [36]. HPU was used as a preparation method due to its efficiency in obtaining homogeneous and stable nanoemulsions [22].

A first experimental design (Design 1, Table 1) was carried out to identify the best balance among oil, surfactants and water percentages. The factors were varied in the following ranges: 4–23% w/w of surfactant, 4–23% w/w of oil, and 54–92% w/w of water. A total of 11 formulations were generated, including three replicated centre points. Formulations N9, N10, and N11 were prepared using a frequency of 20 kHz by varying both amplitude (30 and 40%) and sonication time (5, 10, and 15 min). An amplitude of 40% was initially tested for 5 min; however, excessive sample heating was observed, and longer processing times were therefore avoided to prevent potential AZM thermal degradation. A further optimization consisted of using 30% amplitude, changing the sonication time (5, 10, and 15 min). DLS analysis (Table 1S of Supplementary material) revealed no significant differences in droplet size or PDI among the tested conditions (5, 10 and 15 min; 30 % of amplitude). To reduce the risk of AZM degradation caused by ultrasound, the lowest amplitude (30%) and shortest sonication time (5 min) were chosen to produce a homogeneous and reproducible nanoemulsion. The optical microscope images (Fig. 1S, Supplementary materials) showed that the nanoemulsion achieved after HPU treatment was homogeneous. Hydrodynamic diameter (HD) and PDI were used to prepare and characterize all formulations.

The results obtained revealed that both HD and PDI increased proportionally as the oil and surfactant % increase. The increase in water content, on the other hand, is responsible for the formation of small and homogeneous droplets. Using low surfactant and oil concentrations, the

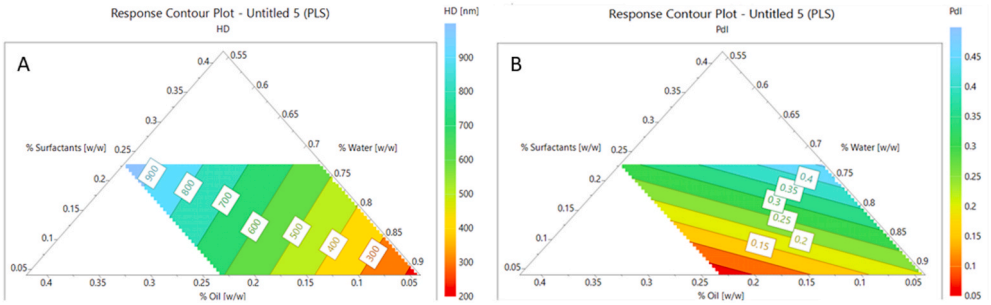

Fig. 1. Desirability plot showing **A**) the HD variation depending on oil, surfactants, water (%w/w), **B**) PDI variation depending on oil, surfactants, water (%w/w).

optimal region (red), corresponding to the lowest HD and PDI values, was identified in the obtained desirability plots (Fig. 1A and B). However, this region is associated with very low oil amount, which would inherently limit AZM solubilization and consequently the total final loading. Therefore, the selection of the most suitable formulation was based not only on minimizing droplet size and PDI, but also on balancing these parameters with an adequate oil fraction to ensure sufficient AZM amount in solution. Among all tested samples, formulation N4 exhibited the most favourable characteristics: mean droplet diameter 726 nm, PDI 0.02, and AZM loading 46 mg/20 mL (Table 4). The statistical evaluation of Design 1 showed that a reliable predictive model was obtained only for PDI ($R^2 = 0.73$; $Q^2 = 0.42$), whereas HD ($R^2 = 0.41$; $Q^2 = 0.25$) exhibited limited predictive ability despite the high reproducibility values. These findings indicated that the explored experimental domain required a refinement; thus, a second experimental design (Design 2, Table 2) was performed to improve the formulation. Considering that high surfactant concentrations lead to both HD and PDI increase, the range of this parameter was narrowed, while the oil fraction was increased to improve AZM loading. Thus, the investigated ranges were: 4–5% by weight of surfactant, 23–41% by weight of oil, and 54–73% by weight of water. The results of this second optimization step (Fig. 2A–B) indicated that formulations N3 and N7 provided the best balance between droplet size and distribution (Table 5). Both samples exhibited mean diameters of approximately 700 nm and low PDI values (0.02 for N3 and 0.04 for N7). Their compositions were similar: N7: 4.5% w/w surfactant, 23% w/w oil and 72.5% w/w water, while N3: 5% w/w surfactant, 23% w/w oil, and 72% w/w water. Even in this case, the obtained data clearly show that both PDI and HD were minimized in formulations containing relatively low surfactant concentrations (approximately 4–5% w/w) and moderate oil content (around 23–25% w/w), combined with a high-water proportion (≥70% w/w). This trend shows the key role of water in promoting droplet dispersion and size uniformity. Both high surfactant and oil amounts lead to increased coalescence and droplet growth [37]. The main statistical parameters derived from the ANOVA analysis and model fitting for both responses of Design 2 were summarized in Table 2S (Supplementary Material). The model-fitting parameters showed that the HD model was statistically significant ($p = 0.034$), with $R^2 = 0.572$ and $Q^2 = 0.456$, and a non-significant lack-of-fit ($p = 0.159$), confirming good model adequacy. For PDI, the model exhibited $R^2 = 0.61$ and $Q^2 = 0.45$, indicating acceptable predictive ability and low experimental variability.

The optimized setpoint predicted by Design 2 was considered the most suitable composition to achieve the desired responses (Fig. 3). These points, indicated by the black circle in both contour plots, represent the predicted composition that, at the same time, satisfies the criteria of minimal PDI and HD and oil amount suitable to ensure adequate AZM solubilization. This predicted condition corresponded to the experimental formulation (hereinafter called AZM_N*) having the following composition: 3.69% w/w Sol, 1.23% w/w SL, 23.00% w/w pumpkin seed oil, 72.08% w/w of ultrapure water containing an amount of AZM corresponding to 2.3 mg/mL.

UHPLC-MS analysis was performed to verify the effect of HPU treatment on AZM stability. Specifically, 3 mL of the optimized AZM_N* nanoemulsion was placed in a dialysis bag and immersed in 200 mL of a water–MeOH (50:50 v/v) to ensure sink conditions. Samples were collected at predetermined intervals (1, 2, 5, 7, and 9 days) and analyzed according to the procedure described in section 2.7. The obtained results showed that the AZM molecular structure is not compromised during HPU treatment (Fig. 2S, Supplementary material) and that the amount of drug entrapped in the oil droplets matched the theoretical loading of 2.3 mg/mL (Table 3S, Supplementary material), confirming that HPU did not induce drug degradation or loss. This result also demonstrates the high entrapment efficiency of the developed system and the chemical compatibility between AZM and the excipients. Finally, the combination of optimal density, complete drug recovery, and chemical stability supported the reliability of the preparation process (HPU). This is important to pose the rationale for conducting accelerated and long-term stability studies for the validation of the formulation's robustness. From the perspective of performing an industrial production of the developed nanoemulsion, it should be considered that one of the main limitations of HPU scaling up is represented by the difficulties in reproducing the ultrasonic amplitudes [38]. This problem can be overcome by barbell horn ultrasonic technology (BHUT), introduced for ultrasonic processes scaling up [38,39].

Overall, the model confirmed the reliability of the experimental design, identifying a formulation that achieves a favourable compromise between droplet uniformity, physical stability, and high drug solubilization capacity, key aspects for the development of stable oral emulsions suitable for pediatric administration.

To highlight the goodness of the developed formulation, in terms of the total amount of AZM solubilized, another experiment was planned, aiming to measure the amount of AZM in solution from the commercial suspension (200 mg/5 mL). Thus, 209.6 mg of AZM dihydrate (corresponding to 200 mg of anhydrous AZM) were dispersed in 5 mL of ultrapure water at 37 °C, under magnetic stirring for 30 min, and then centrifuged (4000 rpm, 10 min). The final concentration in the supernatant was 0.16 mg/mL, ~20-fold lower than that measured in AZM_N* (46 mg/20 mL of nanoemulsion), suggesting the suitability of the developed formulation for drug solubilization improvement.

Table 4
Dimensional values and ζ - Potential of the prepared nanoemulsions by the Design 1.

Sample	HD (nm) ± SD	PDI	ζ-Pot (mV) ± SD	AZM (mg)
N1	862.90 ± 59.46	0.36 ± 0.07	−34.67 ± 2.45	46.0
N2	225.30 ± 16.76	0.22 ± 0.03	−27.92 ± 2.56	10.0
N3	466.50 ± 46.60	0.55 ± 0.07	−33.15 ± 2.59	10.0
N4	726.10 ± 31.94	0.02 ± 0.06	−19.81 ± 3.51	46.0
N5	664.20 ± 23.18	0.11 ± 0.03	−29.18 ± 0.87	27.0
N6	1411.90 ± 67.84	0.22 ± 0.01	−29.35 ± 0.32	30.0
N7	167.90 ± 78.42	0.22 ± 0.05	−26.68 ± 6.80	10.0
N8	588.90 ± 12.57	0.11 ± 0.09	−25.74 ± 3.59	46.0
N9	369.80 ± 17.83	0.29 ± 0.04	−30.95 ± 1.54	28.4
N10	377.50 ± 190.28	0.254	−31.06 ± 2.07	28.4
N11	404.20 ± 197.67	0.239	−28.78 ± 1.61	28.4

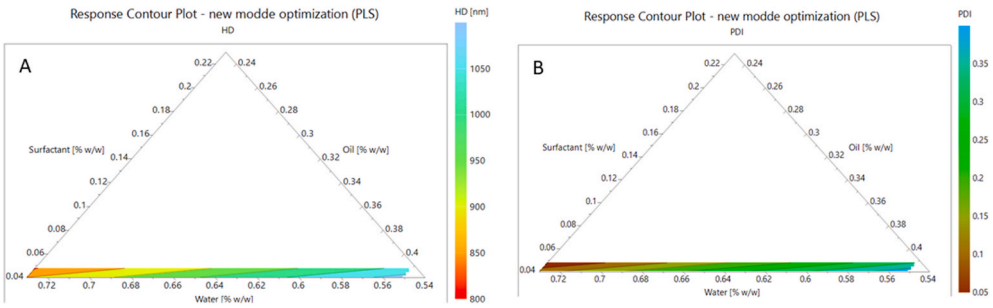

Fig. 2. Desirability plot showing **A**) the HD variation depending on oil, surfactants, water (%w/w), **B**) PDI variation depending on oil, surfactants, water (%w/w).

Table 5
Results of emulsions characterization by the Design 2.

Sample	HD (nm) ± SD	PDI	ζ-Pot (mV) ± SD	AZM (mg)
N1	1000.50 ± 43.21	0.21 ± 0.05	−23.30 ± 1.67	82.0
N2	842.10 ± 55.96	0.09 ± 0.02	−32.48 ± 1.72	46.0
N3	766.10 ± 19.54	0.02 ± 0.06	−27.29 ± 0.63	46.0
N4	988.90 ± 51.24	0.26 ± 0.04	−24.93 ± 2.23	82.0
N5	1024.70 ± 58.42	0.34 ± 0.06	−26.66 ± 0.35	64.0
N6	882.90 ± 39.92	0.14 ± 0.08	−17.61 ± 1.92	64.0
N7	705.30 ± 15.87	0.04 ± 0.06	−29.83 ± 1.76	64.0
N8	983.80 ± 75.65	0.58 ± 0.10	−24.08 ± 3.14	82.0
N9	1041.60 ± 43.09	0.15 ± 0.06	−26.83 ± 5.91	64.0
N10	1059.20 ± 36.14	0.16 ± 0.07	−24.69 ± 2.49	64.0
N11	981.30 ± 38.56	0.158	−23.03 ± 0.74	64.0

3.2. Characterization of the optimized nanoemulsion

AZM_N* submitted to dimensional analysis showed a mean droplet diameter around 800 nm and a narrow size distribution, suggesting the formation of a kinetically stable nanoemulsion, suitable for oral administration.

Although nanoemulsions are often characterized by droplet size less than 500 nm, the upper size limit is not strictly defined and extends up to 1000 nm in several literature reports [40,41]. However, the classification is not just based on the droplet size, but is also influenced by the thermodynamic stability, preparation method, composition and optical properties. The developed system can be appropriately classified as a nanoemulsion, requiring high-energy ultrasonication for the production and relatively low surfactant concentrations. Moreover, exhibited a lactescent appearance and presented droplet sizes in the 700–800 nm range, below the micrometric threshold typical of macroemulsions [42,43].

The morphological analysis was carried out by TEM analysis on the droplets before and after HPU treatment (Fig. 4A–B, respectively).

In the pre-sonication sample (Fig. 4A), the oil droplets appear rather large and polydisperse with poorly defined boundaries, a consequence of the limited energy input and incomplete droplet breakup. After HPU treatment (Fig. 4B), a reduction in droplet size can be detected, together to a narrower size distribution and more uniform spherical contours. This means that acoustic cavitation efficiently disrupted the large oil domains, promoting the formation of smaller and more stable nanodroplets [44]. Furthermore, the predominance of spherical structures could be due to the surfactant system used. Indeed, SL tends to form stable lamellar interfacial films, while Sol, an amphiphilic polymer, provides steric stabilization and improves interfacial elasticity. In addition, these surfactants could promote the formation of well-defined spherical droplets and reduce the likelihood of deformation or coalescence phenomena [45,46]. Overall, the TEM analysis confirms the role of HPU in size reduction, the contribution of the SL–Sol system to droplet morphology. Notably, the droplet diameters observed in the TEM

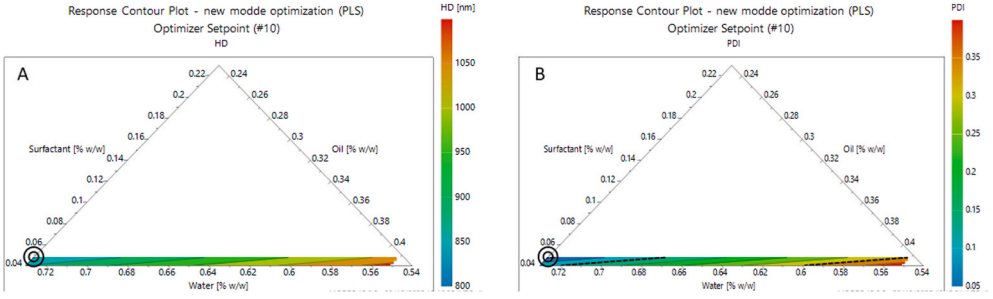

Fig. 3. The optimizer setpoint predicted by Design 2.

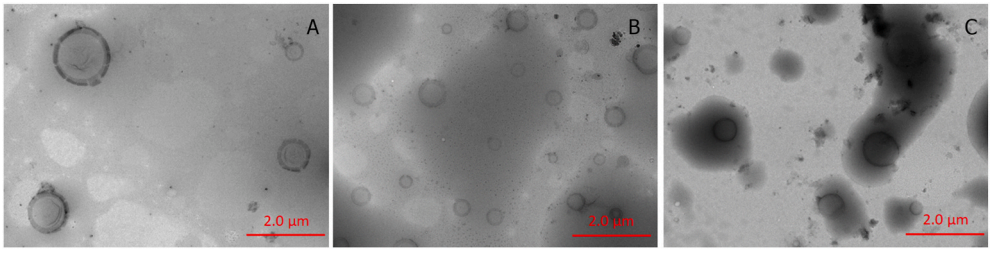

Fig. 4. TEM images of the nanoemulsion **A**) before HPU treatment; **B**) after HPU treatment; **C**) after HPU treatment added by NHB (AZM_N*_NHB). Magnification 7.0k, scale bar 2.0 µm.

images are in good agreement with DLS results, which indicate an average hydrodynamic diameter of approximately 700 nm, confirming the consistency between microscopic and scattering-based measurements.

The nanoemulsion composition was then improved by introducing hydrophilic bentonite nanoclay (NHB) in the external aqueous phase. Bentonite is a hydrated alumina-silicate clay used in the pharmaceutical field for many applications, such as filler, emulsifying agent [47–49]. It is also used as a thickening agent due to the ability to form a gel, once dispersed in water, thanks to the colloidal properties [50,51]. Thus, its introduction in the nanoemulsion was considered useful for further stabilization of the system by increasing the viscosity of the external W phase, as well as the possible interactions between bentonite particles and the surfactant film around the droplets could improve the rheological behaviour of the formulation, reducing creaming or phase separation during storage [52]. Another aspect that guided the choice to introduce NHB in the formulation is AZM's bitter taste. As the taste remains a critical factor affecting compliance, especially in pediatrics, minimal improvements in perceived taste can support adherence to the therapy without compromising formulation stability [53,54]. In this context, it was considered useful to exploit the documented NHB capability to mask the taste of bitter substances, preventing their contact with the specific receptors on human papillae [55]. NHB has been used for many years in the pharmaceutical and food industries and is thus considered safe for use even in pediatrics [56]. A recent study demonstrated bentonite's ability to protect gut microbiota, with benefits against the destabilization induced by antibiotic therapies [57]. This suggests that NHB introduction in the formulation could also be useful for limiting the destabilization of gut flora associated with AZM therapy. TEM analysis, performed on AZM_N* added by NBH (AZM_N*_NHB), indicated the structural modifications induced by clay incorporation. The micrograph (Fig. 4C) reveals a marked structural organization change; the droplets appear associated with darker, irregular clay aggregates, suggesting interactions between the nanodroplets and the bentonite layers. This may involve adsorption, partial encapsulation, or network entrapment within the clay matrix [49].

The ζ-potential of the optimized formulation was also evaluated to assess the electrostatic stability. AZM_N*, without NHB, exhibited a negative ζ-potential of approximately −30 mV, mainly due to the ionized phosphate groups of SL and the anionic contribution of Sol at neutral pH [58,59]. Such a value is generally considered sufficient to ensure repulsive electrostatic forces between droplets, thus preventing coalescence and aggregation over time [60]. After NHB incorporation, the ζ-potential measured was within the same range (−28 mV), indicating that clay introduction does not interfere with the interfacial charge distribution or colloidal stability. Therefore, the highly negative surface potential confirms the robustness of the system, supporting the long-term stability of AZM_N*_NHB.

Viscosity, texture, and mouthfeel are recognized determinants of palatability, although no direct relationship between the density of oral liquid formulations and patient acceptability is clearly established in pediatric [61]. In a patient-centric design framework, the physical parameters of the formulation are often optimized to enhance compliance. In this context, the density of the final nanoemulsion AZM_N*_NHB was measured, obtaining a value equal to 0.9986 g/mL, consistent with typical O/W emulsions and similar to that of pure water (0.98–1.05 g/mL). This parameter is relevant not only from a physical standpoint but also for the sensory perception. Formulations with moderate density are generally associated with good mouthfeel and swallowing comfort, particularly in pediatric patients. Therefore, despite the presence of an oil phase, the developed nanoemulsion can be considered organoleptically acceptable as comparable to conventional aqueous suspensions [62].

3.3. Stability studies

Emulsions, by their nature, are prone to instability phenomena such as phase separation, creaming, and coalescence, which can compromise their performance and shelf-life. To assess the stability of the developed nanoemulsion, both accelerated stress tests and long-term storage studies were performed.

3.3.1. Accelerated stability tests

According to section 2.10, three stress protocols were applied to the optimized AZM_N* nanoemulsion:

1) centrifugation at 4000 rpm for 30 min at RT,
2) heating–cooling cycles (3 ×): alternation between 4 °C and 40 °C, 48 h at each temperature per cycle,
3) freeze–thaw cycles (3 ×): 48 h at 20 °C followed by 48 h at RT per cycle.

These assays aimed to identify early signs of physical instability, such as phase discontinuity, colour changes, gas evolution or sedimentation. After centrifugation, a thin brown layer was observed at the bottom of the flask, attributed to the partial NHB sedimentation, likely due to its higher density relative to the aqueous medium (Fig. 3S, Supplementary material).

During the heating–cooling cycles, phase separation was evident after the second cycle, with the appearance of larger oil droplets and partial coalescence (Fig. 4S, Supplementary material). Freeze–thaw cycles caused more pronounced instability, including colour changes after the first cycle and progressive phase separation from the second cycle onwards (Fig. 5S, Supplementary material). The results are in line with the well-known tendency of emulsions to temperature-induced viscosity changes and interfacial stress. The phase separation observed during accelerated stability tests occurred under stress conditions specifically designed to challenge the system's physical stability. Such tests (e.g., exposure to elevated temperatures or mechanical stress) are routinely employed to identify potential instability mechanisms and assess formulation robustness. However, these experimental settings do not reflect normal pharmaceutical storage or handling conditions. Therefore, the observed phase separation should be interpreted as a stress-induced destabilization phenomenon rather than an indicator of limited real-time shelf stability, useful to define the physical limits of the formulation.

3.3.2. Long-term stability assay

To further evaluate the storage stability, AZM_N*_NHB was kept for 90 days under three controlled temperature conditions: 4 °C, 25 °C, and 40 °C. Samples were analyzed at 30, 60, and 90 days monitoring HD, PDI and ζ-potential (Fig. 5). Throughout the observation period, all samples maintained consistent droplet size and homogeneity. The mean HD remained between 800 and 880 nm under all conditions, while PDI values never exceeded 0.13, confirming the absence of droplet aggregation or coalescence. The slight stabilization observed is attributable to NHB presence, which increases the viscosity of the continuous phase, hindering both droplet movements and creaming [48,63]. The ζ-potential exhibited a gradual decrease over time, from an initial value of −28.00 mV to −9.77 mV at 40 °C, −12.94 mV at 25 °C, and −15.74 mV at 4 °C. This reduction in surface charge may result from cationic adsorption on the bentonite surface as described by Park et al., leading to partial neutralization of the negative charges contributed by SL and Sol [64]. Despite this trend, all values were within the range typical of electrostatically stabilized emulsions, and no visual or dimensional instability was detected. Moreover, it must be underlined that although ζ-potential values decreased to approximately −10 mV at 40 °C, this parameter alone does not fully determine the colloidal stability of the system. In fact, the presence in the external phase increases viscosity and contributes to the formation of a structured network, reducing droplet

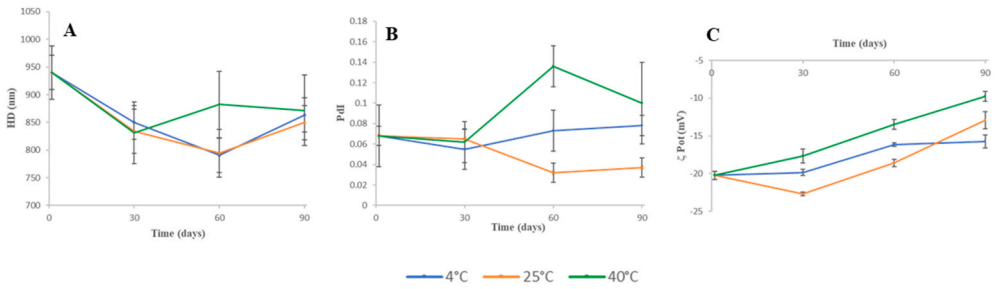

Fig. 5. Measurements performed along 90 days for AZM_N* stored at 4 °C, 25 °C and 40 °C, results of **A**) HD, **B**) PDI and **C**) ζ Potential.

mobility and limiting coalescence. This structural stabilization likely compensates for the reduced electrostatic repulsion [65]. Moreover, no relevant variations in droplet size or PDI were observed during the stability study, confirming the overall physical stability of the formulation and no visual or dimensional instability was detected thanks to the combined contribution of electrostatic and structural stabilization mechanisms.

In general, these results confirm that the developed nanoemulsion AZM_N*_NHB is a physically stable system, for at least three months when stored at 4 °C, 25 °C, and 40 °C, as confirmed by the absence of visual instability and by minimal changes in HD, PDI, and ζ-potential. However, 4 °C and 25 °C represent the most realistic storage conditions for a potential pharmaceutical product and were thus considered the most relevant from a practical standpoint. Moreover, the moderate decrease in ζ -potential at high temperatures suggests minor interfacial rearrangements, although not sufficient to induce phase breakdown. It could be stated that NHB presence contributes positively to nanoemulsions' stabilization. TEM micrographs show that bentonite crystals are dispersed in the external phase represented by the shadows detectable in Fig. 4C. Thus, taking into account that bentonite is not exfoliated, the possible interactions with the oil phase are negligible, but its presence in the water phase is responsible for an increase in the viscosity that could contribute to the physical stabilization of the dispersed droplets. The formulation, therefore, demonstrates adequate stability for further pharmaceutical development and scale-up.

3.4. Gastrointestinal stability and release profile

AZM is known to undergo degradation under acidic conditions, compromising its oral bioavailability [66]. For this reason, the stability of the AZM-loaded nanoemulsion AZM_N*_NHB was firstly studied in SGF pH 1.2 to evaluate the formulation capability to protect the drug from degradation during the gastric transit.

After 30 min of exposure to SGF, followed by neutralization to intestinal pH the dispersion was subjected to dialysis using water/EtOH (50:50 v/v) as medium for up to 9 days to assess the presence of intact AZM. After 72 h, UV analysis of the external medium showed 100% drug recovery; the result was confirmed at subsequent time points (120 h and beyond), indicating that no detectable degradation occurred during acidic exposure (Table 6). These results suggest that the nanoemulsion can protect against acid-induced degradation, preserving the integrity of the active ingredient entrapped in the oil droplets not directly exposed to the acidic medium. These results confirm that the well-known nanoemulsion-based strategy could enhance the oral bioavailability of hydrophobic/acid-sensitive drugs [67]. These findings suggest that by the nanoemulsion, the total AZM administered dose can totally reach the intestine (AZM absorption window [68]) with consequent better absorption.

Table 6
Recovery of AZM from the nanoemulsion after exposure to SGF, pH 1.2 for 30 min followed by pH neutralization and dialysis. Values are expressed as mean ± SD (n = 3).

Time (days)	AZM recovered (%)
1	98.0 ± 0.8
3	100.0 ± 1.2
5	99.0 ± 0.7
7	100.0 ± 0.5
9	100.0 ± 0.9

Based on this evidence, AZM *in vitro* release behaviour from AZM_N*_NHB was evaluated in SIF and compared to an AZM suspension at the same drug concentration (2.3 mg/mL). During the initial phase (up to approximately 60 min), both systems exhibited comparable release profiles (Fig. 6). However, in the subsequent time points, some differences emerged. Specifically, after 24 h, the suspension reached a plateau at approximately 65–70% of drug released, while the nanoemulsion achieved a complete drug release (100%). This result is ascribable to the improved drug solubility within the oily droplets and the greater interfacial contact with the release medium, promoting a sustained diffusion. Furthermore, the submicron droplet size (700-800 nm) provides a balanced interfacial area, preventing excessive burst release while ensuring progressive and complete drug availability over time [69]. The obtained results suggest that the developed nanoemulsion not only preserves AZM stability under gastric conditions, but also improves its intestinal release performance compared to the unformulated drug, supporting its suitability for oral delivery.

In contrast, the suspension is likely to suffer from limited drug solubilization and slower dissolution kinetics, resulting in incomplete release. Moreover, it must be underlined that the experiment does not consider AZM (not formulated in nanoemulsion) degradation in the gastric environment. Thus, the dose that effectively reaches the intestine should be considerably lower than that assayed.

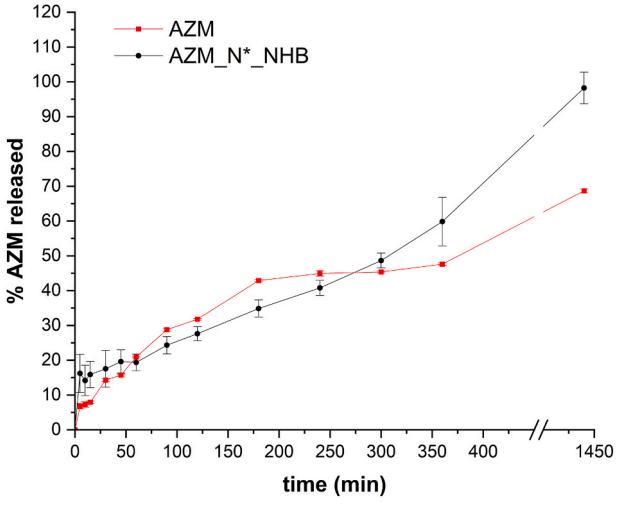

Fig. 6. In vitro release profile of AZM from the nanoemulsion AZM_N*_NHB in SIF pH 6.8/EtOH (80:20 v/v) mixture (n = 3; ±SD). AZM suspension 2.3 mg/mL was used for comparison.

Additionally, it should be noted that the dialysis method used to study the release profiles is a tool for characterizing drug formulation behaviour rather than a direct, real-time simulation of gastrointestinal conditions *in vivo*. It creates a controlled environment and does not fully reproduce the dynamic dilution occurring *in vivo*. Consequently, the release data should be considered indicative of the formulation's diffusion behaviour rather than a direct simulation of gastrointestinal performance [70].

3.5. Antimicrobial activity

The antimicrobial performance of AZM_N*_NHB was firstly evaluated by the agar well diffusion method [71]. Some representative gram-positive bacteria (*S. aureus*, *S. epidermidis*, *S. pyogenes*, *C. perfringens*) were selected, as responsible for many human infections for which AZM is prescribed [72], including in pediatrics [73–77].

The aim was to determine if AZM, introduced in the nanoemulsion (AZM_N*_NHB), maintains its antimicrobial activity. The commercial suspension (200 mg/5 mL) and unloaded emulsion (called N*) were included in the study for comparison.

The obtained results (Table 3) showed that AZM_N*_NHB is active against the tested strains, while no inhibition halos were observed for both unloaded nanoemulsion (N*) and water (negative control), confirming that the antimicrobial effect was exclusively attributable to the incorporated drug. The inhibition halo obtained from the commercial suspension resulted in a larger size than AZM_N*_NHB (Table 3), ascribable to the different amount of AZM in the two products. In fact, considering that 50 μL of each sample was incubated, this volume corresponded to 0.115 mg of AZM completely solubilized for AZM_N*_NHB and to 2 mg for the commercial suspension.

To further explore the effect of AZM_N*_NHB, a time–kill assay was performed using *S. aureus* as a representative strain. As shown in Fig. 7, the nanoemulsion achieved a complete suppression of bacterial growth within 8 h, practically superimposable on that observed for the commercial suspension. Remarkably, these results were obtained using two different AZM concentrations: 23 μg/mL for AZM_N*_NHB and 400 μg/mL for the commercial suspension.

Studies reported in the literature show the improved efficacy of active ingredients formulated in nanoemulsions. The small droplets, in which the drug is dissolved, show a high stability and dispersibility in the bacterial suspension (compared to the solid particles of the commercial product), allowing better access of the drug to bacterial cells with consequent enhanced antibacterial potency [78–80]. It is plausible to hypothesize that the developed nanoemulsion could enhance AZM bioavailability compared to the commercial suspension, which can reduce the daily dose usually prescribed. Therefore, these results demonstrate that the optimized nanoemulsion retains the characteristic antimicrobial activity of AZM despite its lower drug content.

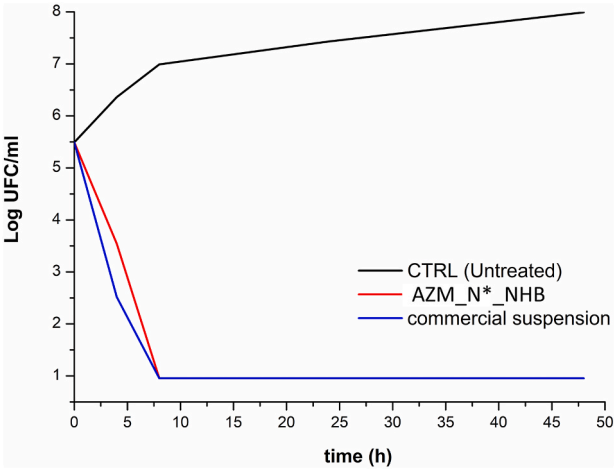

Fig. 7. Estimated growth curves (Log CFU/mL *vs* time) of *S. aureus* incubated with the nanoemulsion AZM_N*_NHB (23 μg/mL) and the commercial suspension (400 μg/mL). CTRL is represented by untreated bacteria.

Although *in vivo* studies should be performed to better understand the bioavailability of the developed formulation, these preliminary results suggest that nanoemulsion-based delivery systems could potentiate the antimicrobial efficacy of poorly soluble antibiotics by improving drug solubilization, dispersion, and interaction with bacterial cells, thereby supporting their potential use as effective oral dosage forms for pediatric therapy.

3.6. In vitro evaluation of AZM binding to TAS2R4 protein

Preliminary studies were performed to evaluate *in vitro* the perception of AZM bitter taste once formulated in the nanoemulsion. It is deeply described in literature that AZM bitter taste perception is due to its interaction with TAS2R4 receptors positioned in the taste buds of the tongue [13]. In our opinion, the developed formulation should have a low bitter taste perception due to i) AZM entrapment in the internal oil phase that could limit the contact with the tongue, ii) bentonite presence that represents a physical barrier able to reduce the contact between AZM and tongue receptors. To support our hypothesis, an *in vitro* experiment was planned to evaluate the interaction between AZM and TAS2R4 receptor, adapting an ELISA assay available on the market. The kit contains antibodies binding TAS2R4 receptor proteins. Thus, using the standard provided with the kit, represented by the protein TAS2R4, a calibration curve was first prepared. Then, solutions of different samples were prepared in the presence of a fixed concentration of TAS2R4 protein (provided in the kit). The tested samples were: i) sucrose (used as negative control), ii) AZM (used as positive control), iii) AZM_N*_NHB.

The OD value is a function of TAS2R4 -antibody binding. This means that if the receptor does not interact with a substrate, it is free to bind the antibody, producing a high OD value.

The obtained results (Fig. 8) show that the OD value measured was high for the sucrose (red bars). This means that, as sucrose is not a substrate, the TAS2R4 protein can bind to the antibody, allowing to measure an appreciable OD value. Lower OD values were recorded for the other samples. The OD value measured for the AZM sample (orange bars) is lower than that of sucrose. This is due to AZM's capacity to bind the protein TAS2R4, which reduces the availability of sites for antibody binding. For AZM_N*_NHB (blue bars), the signal is very low, hypothesizing that TAS2R4-antibody interaction is prevented, as assessed by the low OD values measured.

4. Conclusions

An innovative azithromycin (AZM) oil-in-water nanoemulsion was successfully developed and optimized as a liquid oral formulation suitable for pediatric administration. The formulation strategy was based on combining the natural surfactant soy lecithin with the polymeric synthetic solubilizer Soluplus®, resulting in a system characterized by high solubilizing capacity, homogeneity and good stability. The use of pumpkin seed oil as the internal phase ensured efficient solubilization of the lipophilic drug, allowing a maximum loading of 46 mg/20 mL of nanoemulsion. The formulation does not require reconstitution (precise dosing) and shaking before use, guaranteeing ease of dosing (dose measurement correct). Moreover, it could meet patient acceptability as it was optimized to reduce the interaction between the drug, confined in the oil droplets, and the bitter taste receptors. The introduction of bentonite nanoclay in the external phase is also useful to further reduce this contact.

Taken together, the structural design of the dual-surfactant nanosystem (SL/Sol) combined with a nanoclay component could represent a simple and comprehensive approach to optimize both the physicochemical and patient-centred performance of AZM oral formulations. In

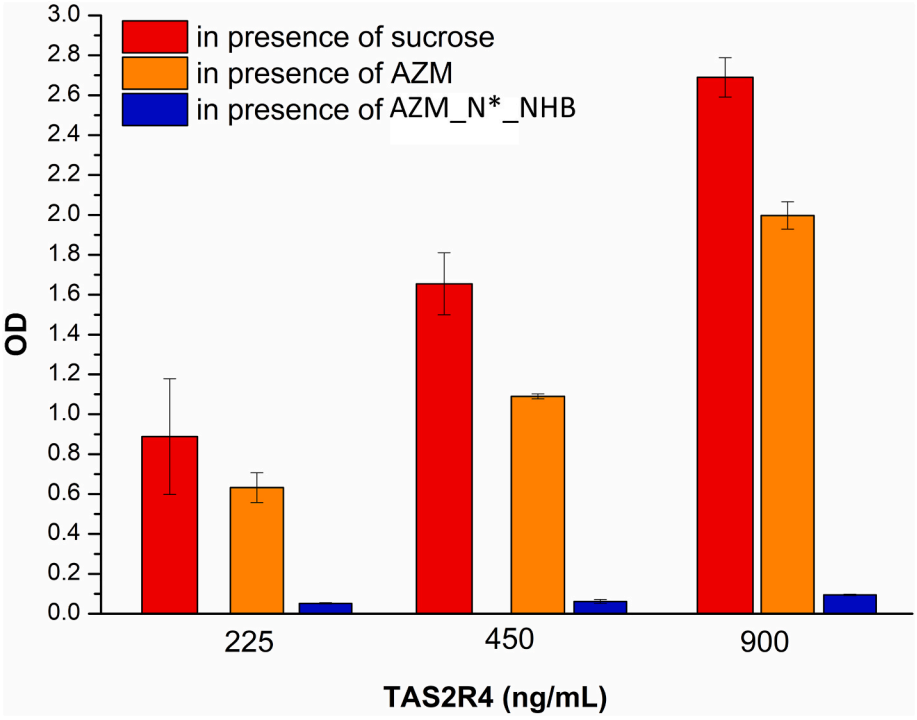

Fig. 8. Results obtained from the ELISA assay.

addition, it is also interesting to highlight that the oral formulation was prepared using: i) simple, easily available and safe excipients, which do not add toxicity to the pharmaceutical preparation, ii) a simple, non-polluting method.

Further studies should be performed to evaluate the *in vivo* performance of the developed formulation, in order to assess its suitability in paediatrics.

Funding

This study is part of the project "3D-printed antibiotic oral dosage forms for paediatric use" [p3Diatrics] under the Project of Relevant National Interest (PRIN 2022) call, funded by Ministero dell'Università e della Ricerca. Project ID: 2022FRNFMT.

CRediT authorship contribution statement

Anna Imbriano: Conceptualization, Data curation, Formal analysis, Investigation, Writing – original draft. **Alessandro Di Michele:** Data curation, Formal analysis, Investigation. **Maria Rachele Ceccarini:** Data curation, Formal analysis. **Angela Abruzzo:** Conceptualization, Funding acquisition, Writing – review & editing. **Federica Bigucci:** Supervision, Writing – review & editing. **Dritan Hasa:** Conceptualization, Funding acquisition, Writing – review & editing. **Ilenia D'Abbrunzo:** Data curation, Formal analysis. **Luca Casettari:** Conceptualization, Funding acquisition, Writing – review & editing. **Costanza Fratini:** Data curation, Formal analysis. **Sara Primavilla:** Data curation, Formal analysis. **Lorenzo Tazza:** Formal analysis. **Leonardo Tensi:** Data curation, Formal analysis. **Luana Perioli:** Supervision, Writing – review & editing. **Cinzia Pagano:** Conceptualization, Funding acquisition, Project administration, Writing – original draft, Writing – review & editing.

Declaration of competing interest

The authors declare that they have no known competing financial interests or personal relationships that could have appeared to influence the work reported in this paper.

Acknowledgements

Authors sincerely acknowledge: Marco Marani from the Department of Pharmaceutical Sciences of the University of Perugia for technical assistance; Ilaria Marinelli from the Department of Biomolecular Sciences of University of Urbino for TEM measurements.

Appendix A. Supplementary data

Supplementary data to this article can be found online at https://doi.org/10.1016/j.jddst.2026.108368.

Data availability

Data will be made available on request.

References

[1] A.E. Girard, D. Girard, A.R. English, T.D. Gootz, C.R. Cimochowski, J.A. Faiella, S. L. Haskell, J.A. Retsema, Pharmacokinetic and in vivo studies with azithromycin (CP-62,993), a new macrolide with an extended half-life and excellent tissue distribution, antimicrob, Agents Chemother. 31 (1987) 1948–1954.
[2] A. Imbriano, C. Fratini, G. Bondi, I. D'Abbrunzo, S. Bertoni, M. Tiboni, A. Abruzzo, D. Hasa, C. Pagano, L. Casettari, A. 3D-printed chewable gummy tablets: a new tool for oral amoxicillin administration in paediatric population, Int. J. Pharm. 677 (2025) 125645.
[3] L. Zeng, P. Xu, I. Choonara, Z. Bo, X. Pan, W. Li, X. Ni, T. Xiong, C. Chen, L. Huang, S.A. Qazi, D. Mu, L. Zhang, Safety of azithromycin in pediatrics: a systematic review and meta-analysis, Eur. J. Clin. Pharmacol. 76 (2020) 1709–1721.
[4] Z. Wang, G. Gan, H. Yao, Gastrointestinal safety of oral erythromycin, clarithromycin, and azithromycin in pediatric patients: a FAERS pharmacovigilance study, Pediatr. Res. 99 (2025) 1051–1059.
[5] S. Hopkins, Clinical safety and tolerance of azithromycin in children, J. Antimicrob. Chemother. 31 (1993) 111–117.
[6] I. D'Abbrunzo, L. Battaiotto, A. Abruzzo, G. Bondi, F. Bigucci, C. Pagano, A. Imbriano, C. Fratini, L. Casettari, D. Voinovich, D. Hasa, Structural insights into novel coamorphous systems of azithromycin with faster dissolution profile, Eur. J. Pharm. Biopharm. 216 (2025) e114873.

[7] M.J. Mora, R. Onnainty, G.E. Granero, Comparative oral drug classification systems: acetazolamide, azithromycin, clopidogrel, and efavirenz case studies, Mol. Pharm. 15 (2018) 3187–3196.
[8] H.D. Langtry, J.A. Balfour, Azithromycin: a review of its use in paediatric infectious diseases, Drugs 56 (1998) 273–297.
[9] J.M. Lieberman, Appropriate antibiotic use and why it is important: the challenges of bacterial resistance, Pediatr. Infect. Dis. J. 22 (2003) 1143–1151.
[10] T. Uchida, Taste sensor assessment of bitterness in medicines: overview and recent topics, Sensors 24 (2024) 4799.
[11] S.R. Ranmal, J. Walsh, C. Tuleu, Poor-tasting pediatric medicines: part 1. A scoping review of their impact on patient acceptability, medication adherence, and treatment outcomes, Front. Drug Deliv. 5 (2025) 1553286.
[12] M. El-Sahn, R. Elliott, M. El-Sahn, I. Lucas, K. Kong, J. Walsh, J. Lucas, Poor-tasting pediatric medicines: part 2. Exploring caregiver and healthcare provider values and preferences for a novel taste-blocker product to improve acceptability, front, Drug Deliv. 5 (2025) 1555522.
[13] A. Jaggupilli, N. Singh, V.C. De Jesus, M.S. Gounni, P. Dhanaraj, P. Chelikani, Chemosensory bitter taste receptors (T2Rs) are activated by multiple antibiotics, FASEB J. 33 (2019) 501–517.
[14] F. Amin, S. Khan, S.M.H. Shah, H. Rahim, Z. Hussain, M. Sohail, R. Ullah, M. S. Alsaid, A.A. Shahat, A new strategy for taste masking of azithromycin antibiotic: development, characterization, and evaluation of azithromycin titanium nanohybrid for masking of bitter taste using physisorption and panel testing studies, Drug Des. Dev. Ther. 12 (2018) 3855–3866.
[15] H. Mashaqbeh, R. Obaidat, M.M. Alsmadi, T. Athamneh, Comparison between solvent evaporation and supercritical CO2 technology in taste-masking of azithromycin bitter-taste using pH-sensitive eudragit EPO or eudragit S100 polymers, J. Appl. Pharmaceut. Sci. 14 (2024) 131–138.
[16] M. Zhao, L. Sheng Wang, H. Wen Liu, Y. Jing Wang, H. Yang, Preparation, physicochemical characterization and in vitro dissolution studies of azithromycin-cyclodextrin inclusion complexes, J. Inclusion Phenom. Macrocycl. Chem. 85 (2016) 137–149.
[17] R. Huang, Y. Zhang, T. Wang, L. Shen, Z. Zhang, Y. Wang, D. Quan, Creation of an assessment system for measuring the bitterness of azithromycin-containing reverse micelles, Asian J. Pharm. Sci. 13 (2018) 343–352.
[18] R.A. Assi, I.M. Abdulbaqi, T.S. Ming, C.S. Yee, H.A. Wahab, S.M. Asif, Y. Darwis, Liquid and solid self-emulsifying drug delivery systems (sedds) as carriers for the oral delivery of azithromycin: optimization, in vitro characterization and stability assessment, Pharmaceutics 12 (2020) 1052.
[19] D.T.M. Huynh, H.T. Hai, N.M. Hau, H.K. Lan, T.P. Vinh, V. De Tran, D.T. Pham, Preparations and characterizations of effervescent granules containing azithromycin solid dispersion for children and elder: solubility enhancement, taste-masking, and digestive acidic protection, Heliyon 9 (2023) e16592.
[20] S. Sambhakar Preeti, R. Malik, S. Bhatia, A. Al Harrasi, C. Rani, R. Saharan, S. Kumar, R. Geeta, Sehrawat, nanoemulsion: an emerging novel technology for improving the bioavailability of drugs, Scientifica (Cairo) 2023 (2023) 6640103.
[21] A. Pratap-Singh, Y. Guo, S. Lara Ochoa, F. Fathordoobady, A. Singh, Optimal ultrasonication process time remains constant for a specific nanoemulsion size reduction system, Sci. Rep. 11 (2021) e9241.
[22] S. Kentish, T.J. Wooster, M. Ashokkumar, S. Balachandran, R. Mawson, L. Simons, The use of ultrasonics for nanoemulsion preparation, Innov. Food Sci. Emerg. Technol. 9 (2008) 170–175.
[23] J. Bhatia, F. Greer, Use of soy protein-based formulas in infant feeding, Pediatrics 121 (2008) 1062–1068.
[24] J.S.U. Tabaniag, M.Q.D. Abad, C.J.R. Morcelos, G.V.B. Geraldino, J.L.M. Alvarado, E.C.R. Lopez, Stabilization of oil/water emulsions using soybean lecithin as a biobased surfactant for enhanced oil recovery, J. Eng. Appl. Sci. 70 (2023) 1–26.
[25] N. Guembe-Michel, P. Nguewa, G. González-Gaitano, Soluplus®-based pharmaceutical formulations: recent advances in drug delivery and biomedical applications, Int. J. Mol. Sci. 26 (2025) 1–28.
[26] J.F. Alopaeus, E. Hagesæther, I. Tho, Micellisation mechanism and behaviour of soluplus®–furosemide micelles: preformulation studies of an oral nanocarrier-based system, Pharmaceuticals 12 (2019) 1–23.
[27] R. Pignatello, R. Corsaro, A. Bonaccorso, E. Zingale, C. Carbone, T. Musumeci, Soluplus® polymeric nanomicelles improve solubility of BCS-Class II drugs, Drug Deliv. Transl. Res. 12 (2022) 1991–2006.
[28] N. Sultana, M.S. Arayne, F. Hussain, A. Fatima, Degradation studies of azithromycin and its spectrophotometric determination in pharmaceutical dosage forms, Pak. J. Pharm. Sci. 19 (2006) 98–103.
[29] T. Kiyota, A. Kambayashi, T. Takagi, S. Yamashita, Importance of gastric secretion and the rapid gastric emptying of ingested water along the lesser curvature ("Magenstraße") in predicting the in vivo performance of liquid oral dosage forms in the fed state using a modeling and simulation, Mol. Pharm. 19 (2022) 642–653.
[30] J. Fallingborg, L.A. Christensen, M. Ingeman-Nielsen, B.A. Jacobsen, K. Abildgaard, H.H. Rasmussen, pH-Profile and regional transit times of the normal gut measured by a radiotelemetry device, aliment, Pharmacol. Ther. 3 (1989) 605–614.
[31] M. Balouiri, M. Sadiki, S.K. Ibnsouda, Methods for in vitro evaluating antimicrobial activity: a review, J. Pharm. Anal. 6 (2016) 71–79.
[32] C.L. Pérez Gutíerrez, A. Di Michele, C. Pagano, D. Puglia, F. Luzi, T. Beccari, M. R. Ceccarini, S. Primavilla, A. Valiani, C. Vicino, M. Ricci, C.A. Viseras Iborra, L. Perioli, Polymeric patches based on chitosan/green clay composites and hazelnut shell extract as bio-sustainable medication for wounds, Pharmaceutics 15 (2023) 1–17.
[33] D.J. McClements, Nanoemulsion-based oral delivery systems for lipophilic bioactive components: nutraceuticals and pharmaceuticals, Ther. Deliv. 4 (2013) 841–857.
[34] A. Nawirska-Olszańska, A. Kita, A. Biesiada, A. Sokół-Łętowska, A.Z. Kucharska, Characteristics of antioxidant activity and composition of pumpkin seed oils in 12 cultivars, Food Chem. 139 (2013) 155–161.
[35] M. SanchezBallester, N.M. Devoisselle, J.M. Bégu, S. Soulairol, I. Monteil, Regulations on excipients used in 3D printing of pediatric oral forms, Int. J. Pharm. 662 (2024) 124402.
[36] S.V. Mangrulkar, S.S. Kulkarni, P.V. Nanepag, P.S. Neje, D.R. Chaple, B. G. Taksande, M.J. Umekar, A comprehensive review on pleiotropic effects and therapeutic potential of soy lecithin, Adv. Tradit. Med. 25 (2025) 145–164.
[37] T. Xiao, X. Ma, H. Hu, F. Xiang, X. Zhang, Y. Zheng, H. Dong, B. Adhikari, Q. Wang, A. Shi, Advances in emulsion stability: a review on mechanisms, role of emulsifiers, and applications in food, Food Chem. X. 29 (2025) e102792.
[38] A.S. Peshkovsky, S. Bystryak, Continuous-flow production of a pharmaceutical nanoemulsion by high-amplitude ultrasound: process scale-up, Chem. Eng. Process. Process Intensif. 82 (2014) 132–136.
[39] A.S. Peshkovsky, From research to production: overcoming Scale-Up limitations of ultrasonic processing, in: Ultrasound Adv. Food Process, Preserv., 2017, pp. 409–423.
[40] D.J. McClements, Nanoemulsions versus microemulsions: terminology, differences, and similarities, Soft Matter 8 (2012) 841–857.
[41] M. Jaiswal, R. Dudhe, P.K. Sharma, Nanoemulsion: an advanced mode of drug delivery system, 3 Biotech 5 (2015) 123–127.
[42] N.H.C. Marzuki, R.A. Wahab, M.A. Hamid, An overview of nanoemulsion: concepts of development and cosmeceutical applications, Biotechnol. Biotechnol. Equip. 33 (2019) 779–797.
[43] V. Changediya, Nanoemulsions: a recent drug delivery tool, in: Des. Appl. Self-Assembly Aggregates - from Micelles to Nanoemulsions, 2024.
[44] T.S.H. Leong, T.J. Wooster, S.E. Kentish, M. Ashokkumar, Minimising oil droplet size using ultrasonic emulsification, Ultrason. Sonochem. 16 (2009) 721–727.
[45] L. Deng, Current progress in the utilization of soy-based emulsifiers in food applications—a review, Foods 10 (2021) 1–18.
[46] H. Mateos, L. Gentile, S. Murgia, G. Colafemmina, M. Collu, J. Smets, G. Palazzo, Understanding the self-assembly of the polymeric drug solubilizer soluplus®, J. Colloid Interface Sci. 611 (2022) 224–234.
[47] S.T. Stojiljković, M.S. Stojiljković, Application of bentonite clay for human use, in: Proc. IV Adv. Ceram. Appl. Conf., 2017, pp. 349–356.
[48] A. Imbriano, M. Mendico, S. Primavilla, M. Carafa, L. Perioli, M. Ricci, A. Di Michele, C. Viseras, C. Pagano, F.G. Villén, R. de Melo Barbosa, Development of nanoemulgel system based on Opuntia ficus-indica (L.) seed oil and nanoclays: formulation, characterization and application for wound treatment, J. Drug Deliv. Sci. Technol. 111 (2025) e107151.
[49] A. Imbriano, F. García-Villén, J. Forte, M. Ruggeri, A. Lasalvia, F. Rinaldi, L. Perioli, G. Sandri, C. Marianecci, C. Viseras, M. Carafa, Clay-carvacrol nanoemulsions for wound healing: design and characterization studies, J. Drug Deliv. Sci. Technol. 99 (2024) e105984.
[50] Y. Lin, H. Qin, J. Guo, J. Chen, Rheology of bentonite dispersions: role of ionic strength and solid content, Appl. Clay Sci. 214 (2021) 106275.
[51] P.F. Luckham, S. Rossi, Colloidal and rheological properties of bentonite suspensions, Adv. Colloid Interface Sci. 82 (1999) 43–92.
[52] C. Viseras, R. Sánchez-Espejo, R. Palumbo, N. Liccardi, F. García-Villén, A. Borrego-Sánchez, M. Massaro, S. Riela, A. López-Galindo, Clays in cosmetics and personal care products, Clays Clay Miner. 69 (2021) 561–575.
[53] H.M. Schluterman, C.G. Linardos, T. Drulia, J.D. Marshall, G.L. Kearns, Evaluating palatability in young children: a mini-review of relevant physiology and assessment techniques, Front. Pediatr. 12 (2024) e1350662.
[54] G. Bondi, I. D'Abbrunzo, D. Hasa, C. Parolin, B. Vitali, S. Bertoni, A. Imbriano, C. Pagano, C. Fratini, B. Sabbatini, F. Bigucci, A. Abruzzo, Innovative bilayered buccal films: a paediatric-friendly dosage form for transmucosal azithromycin delivery, Int. J. Pharm. 684 (2025) e126164.
[55] J.H. Lee, G. Choi, Y.J. Oh, J.W. Park, Y. Bin Choy, M.C. Park, Y.J. Yoon, H.J. Lee, H.C. Chang, J.H. Choy, A nanohybrid system for taste masking of sildenafil, Int. J. Nanomed. 7 (2012) 1635–1649.
[56] M.K. Ng, D.J. Jacofsky, W.K. Barsoum, M.A. Mont, Human health applications of calcium montmorillonite clay: a systems-based review, Cureus (2025) e95449.
[57] R. Heydari, R. Abiri, H. Rezaee-Shafe, Evaluating bentonite clay's potential in protecting intestinal flora and alleviating pseudomembranous colitis following antibiotic usage, Med. Hypotheses 191 (2024) 111443.
[58] E.M. Tomou, P. Papakyriakopoulou, E.M. Saitani, G. Valsami, N. Pippa, H. Skaltsa, Recent advances in nanoformulations for Quercetin delivery, Pharmaceutics 15 (2023) 1656.
[59] R.S. Schuh, F. Bruxel, H.F. Teixeira, Physicochemical properties of lecithin-based nanoemulsions obtained by spontaneous emulsification or high-pressure homogenization, Quim. Nova 37 (2014) 1193–1198.
[60] T.L. Doane, C.H. Chuang, R.J. Hill, C. Burda, Nanoparticle ζ -potentials, Acc. Chem. Res. 45 (2012) 317–326.
[61] F. Liu, S. Ranmal, H.K. Batchelor, M. Orlu-Gul, T.B. Ernest, I.W. Thomas, T. Flanagan, R. Kendall, C. Tuleu, Formulation factors affecting acceptability of oral medicines in children, Int. J. Pharm. 492 (2015) 341–343.
[62] J.D.N. Ogbonna, E. Cunha, A.A. Attama, K.C. Ofokansi, H. Ferreira, S. Pinto, J. Gomes, Í.M.G. Marx, A.M. Peres, J.M.S. Lobo, I.F. Almeida, Overcoming challenges in pediatric formulation with a patient-centric design approach: a proof-of-concept study on the design of an oral solution of a bitter drug, Pharmaceuticals 15 (2022) 1–14.

[63] N. Querol, C. Barreneche, L.F. Cabeza, Storage stability of bimodal emulsions vs. monomodal emulsions, Appl. Sci. 7 (2017) 1–15.
[64] J.H. Park, H.J. Shin, M.H. Kim, J.S. Kim, N. Kang, J.Y. Lee, K.T. Kim, J.I. Lee, D. D. Kim, Application of montmorillonite in bentonite as a pharmaceutical excipient in drug delivery systems, J. Pharm. Investig. 46 (2016) 363–375.
[65] J.S. Hong, P. Fischer, Bulk and interfacial rheology of emulsions stabilized with clay particles, Colloids Surfaces A Physicochem. Eng. Asp. 508 (2016) 316–326.
[66] M.G. Saita, D. Aleo, B. Melilli, S. Mangiafico, M. Cro, C. Sanfilippo, A. Patti, pH-Dependent stability of azithromycin in aqueous solution and structure identification of two new degradation products, J. Pharm. Biomed. Anal. 158 (2018) 47–53.
[67] M. Saha, A. Gupta, S. Kunkalienkar, N. Dhas, S. Shetty, A. Gupta, S. Mutalik, N. Krishnadas, R. Chandrashekar, N. Narasimhaswamy, S. Moorkoth, Nanoemulsion as a promising drug delivery strategy for effective eradication of helicobacter pylori: current insights, Drug Deliv. Transl. Res. 16 (2026) 17–44.
[68] E. Garver, E.D. Hugger, S.P. Shearn, A. Rao, P.A. Dawson, C.B. Davis, C. Han, Involvement of intestinal uptake transporters in the absorption of azithromycin and clarithromycin in the rat, Drug Metab. Dispos. 36 (2008) 2492–2498.
[69] S. Jacob, F.S. Kather, S.H.S. Boddu, J. Shah, A.B. Nair, Innovations in nanoemulsion technology: enhancing drug delivery for oral, parenteral, and ophthalmic applications, Pharmaceutics 16 (2024) 1333.
[70] M. Yu, W. Yuan, D. Li, A. Schwendeman, S.P. Schwendeman, Predicting drug release kinetics from nanocarriers inside dialysis bags, J. Contr. Release 315 (2019) 23–30.
[71] S. Primavilla, C. Pagano, R. Roila, R. Branciari, D. Ranucci, A. Valiani, M. Ricci, L. Perioli, Antibacterial activity of crocus sativus L. petals extracts against foodborne pathogenic and spoilage microorganisms, with a special focus on Clostridia, Life 13 (2023) 60.
[72] J.M. Pieniążek, A. Padkowska, M. Dobosz, K. Arciszewska, J. Buczkowski, M. Miazga, M. Paprocki, A. Mataczyńska, Overview of the main bacterial infections in humans, Qual. Sport. 23 (2024) 54786.
[73] A.J. Campbell, L.S. Al Yazidi, L.K. Phuong, C. Leung, E.J. Best, R.H. Webb, L. Voss, E. Athan, P.N. Britton, P.A. Bryant, C.T. Butters, J.R. Carapetis, N.S. Ching, G. W. Coombs, D.A. Daley, J.R. Francis, T.Y. Hung, S. Mowlaboccus, C. Nourse, S. Ojaimi, A. Tai, N. Vasilunas, B. McMullan, C.C. Blyth, A.C. Bowen, Pediatric Staphylococcus aureus bacteremia: clinical spectrum and predictors of poor outcome, Clin. Infect. Dis. 74 (2022) 604–613.
[74] A. Trobisch, N.A. Schweintzger, D.S. Kohlfürst, M.G. Sagmeister, M. Sperl, A. J. Grisold, G. Feierl, J.A. Herberg, E.D. Carrol, S.C. Paulus, M. Emonts, M. van der Flier, R. de Groot, M. Cebey-López, I. Rivero-Calle, N.P. Boeddha, P.M. Agapow, F. Secka, S.T. Anderson, U. Behrends, U. Wintergerst, K. Reiter, F. Martinon-Torres, M. Levin, W. Zenz, Osteoarticular infections in pediatric hospitals in Europe: a prospective cohort study from the EUCLIDS consortium, Front. Pediatr. 10 (2022) 744182.
[75] I.A. Joubert, M. Otto, T. Strunk, A.J. Currie, Look who's talking: host and pathogen drivers of Staphylococcus epidermidis virulence in neonatal sepsis, Int. J. Mol. Sci. 23 (2022) 860.
[76] D. Espadas Maciá, E.M. Flor Macián, R. Borrás, S. Poujois Gisbert, J.I. Muñoz Bonet, Streptococcus pyogenes infection in paediatrics: from pharyngotonsillitis to invasive infections, An. Pediatr 88 (2018) 75–81.
[77] I. Brook, Clostridial infections in children: spectrum and management, Curr. Infect. Dis. Rep. 17 (2015) 47.
[78] H. Yazgan, Y. Ozogul, E. Kuley, Antimicrobial influence of nanoemulsified lemon essential oil and pure lemon essential oil on food-borne pathogens and fish spoilage bacteria, Int. J. Food Microbiol. 306 (2019) 108266.
[79] S. Garzoli, S. Petralito, E. Ovidi, G. Turchetti, V. Laghezza Masci, A. Tiezzi, J. Trilli, S. Cesa, M.A. Casadei, P. Giacomello, P. Paolicelli, Lavandula x intermedia essential oil and hydrolate: evaluation of chemical composition and antibacterial activity before and after formulation in nanoemulsion, Ind. Crops Prod. 145 (2020) 112068.
[80] M. Liu, Y. Pan, M. Feng, W. Guo, X. Fan, L. Feng, J. Huang, Y. Cao, Garlic essential oil in water nanoemulsion prepared by high-power ultrasound: properties, stability and its antibacterial mechanism against MRSA isolated from pork, Ultrason. Sonochem. 90 (2022) 106201.